

Polymorphism in Bis(4-dimethylamino-pyridinium)tetrachlorocuprate(II)

Salim Haddad

Department of Chemistry, The University of Jordan,
Amman, Jordan

Roger D. Willett*

Department of Chemistry, Washington State University,
Pullman, Washington 99164

Received June 6, 2000

Introduction

Polymorphism in solid-state structures is a common phenomenon. The driving forces can be complex, but the observed structures represent different ways of obtaining efficient packing of the components of the structure. In transition metal compounds, this effect is often evident by the observation of different colors associated with the different isomorphs. In our laboratory, this has led to the study of thermochromism¹ and piezochromism, particularly in copper(II) halide salts.² Here the transformation between the different colored isomorphs is triggered by the external stresses of temperature and pressure, respectively. The transformation between phases may be facile, but when the transition is first order, supercooling and superheating are common. Hence, it is possible to have crystals of several isomorphs coexisting under identical conditions.

In our studies of hybrid organic/inorganic materials based on organoammonium salts of copper(II) halides, the role of hydrogen bonding between the organic cations and the copper halide species has been identified as a primary factor influencing the relative stability of various crystalline phases. In the cases where isolated CuCl_4^{2-} anions are found in the lattice, the distortion of the anions can be directly correlated with the strength of this hydrogen bonding. In general, the stronger the hydrogen bonding, the closer the anions are to a square planar coordination.³ Presumably, this is due to a reduction of the effective charge on the chloride ions, thus reducing the electrostatic repulsion between the Cl^- ions within the CuCl_4^{2-} species. The weakening of the hydrogen bonding in the lattice has usually been associated with the onset of disorder of the organic cations driven by the increased thermal energy at higher temperatures.^{1a}

The situation is more complicated in cases where extended copper halide networks exist. Now competition between the hydrogen-bonding interactions and bridging Cu–X–Cu interactions exists. Here the disorder of the organic cations at higher temperatures, and the associated weakening of the hydrogen bonding, can trigger changes in the coordination number for the Cu(II) ions and thus change the connectivity of the extended

Cu halide framework.^{1b,2a,4} This is evidenced by changes in the properties that are sensitive to this connectivity, e.g., magnetic behavior.

In this paper we report on the structure of two isomorphs of the title compound. The two phases can be cocrystallized from solution at room temperature. In addition, no disorder of the organic cation is observed in either phase.

Experimental Section

Preparation of the Complexes. All syntheses were conducted using reagent grade chemicals and were used without further purification with the exception that CuCl was purified by boiling in a solution of ascorbic acid. CuCl and $\text{CuCl}_2 \cdot 2\text{H}_2\text{O}$ were Baker Analyzed (Reagent) from J. T. Baker. 4-(Dimethylamino)pyridine, 99%, and ascorbic acid were from Aldrich. Acetonitrile and HCl were from Fisher ChemAlert(R) Guide.

(a) Yellow Phase: Bis(4-dimethylaminopyridinium)tetrachlorocuprate(II), $(\text{C}_7\text{H}_{11}\text{N}_2)_2\text{CuCl}_4$. The more stable of the two isomers could be obtained from slightly acidic medium (0.1 M HCl) or strongly acidic medium (3 M HCl), be it from ethanol-based solution or acetonitrile-based solution among many. Well-formed parallelepiped-shaped yellow crystals were obtained by heating a solution of 5 mmol of $\text{CuCl}_2 \cdot 2\text{H}_2\text{O}$ and 5 mmol of 4-(dimethylamino)pyridine in 20 mL of 3 M HCl in a beaker for 5 min at 75 °C. Slow evaporation in the open beaker allowed crystals to develop overnight. A single crystal of approximate dimensions 0.3 mm × 0.3 mm × 0.4 mm was used for structure determination.

(b) Green Phase: Bis(4-dimethylaminopyridinium)tetrachlorocuprate(II), $(\text{C}_7\text{H}_{11}\text{N}_2)_2\text{CuCl}_4$. This isomer is not stable under room conditions and turns to the yellow isomer upon standing in air or sitting in the mother liquor. However, it is possible to extend the life span of the isomer by storing it in a dry atmosphere in a desiccator or in a tightly closed vial. Recrystallization of the yellow isomer from 0.1 M HCl by boiling followed by slow evaporation first produced large clusters of mixed crystals of the two isomers. However, the green ones convert to the yellow form within a few hours if left in mother liquor or, at a much slower rate, if removed and stored in a vial.

Good quality longitudinal parallelepiped-shaped green crystals that are well separated were made in excess of the yellow ones when 5 mmol of CuCl , 5 mmol of $\text{CuCl}_2 \cdot 2\text{H}_2\text{O}$, and 5 mmol of 4-(dimethylamino)pyridine are stirred at room temperature in 60 mL of acetonitrile acidified with 6 mL of 1 M HCl. Slow evaporation in the open beaker produced a mixture of discrete green and yellow crystals at the bottom of the beaker under the mother liquor, while only the green isomer formed at the sides of the beaker where the solution was in contact with air. A pure sample of the green crystals was obtained by scraping the sides of the beaker after decantation. A green crystal of dimensions 0.2 mm × 0.3 mm × 0.5 mm cut from a longer crystal was used for structure determination.

Differential Scanning Calorimetry. DSC measurements were performed on the green isomer in the range –60 to 160 °C and at a scanning rate of 10 deg/min shows a phase transition at 120 °C. From –60 °C and up to 120 °C the crystals remained green, but by 123 °C they had all turned yellow.

X-ray Diffraction. Data for the compounds were collected on a Siemens 1000 three-circle platform diffractometer equipped with a CCD detector maintained near –54 °C, and the x axis was fixed at 54.74°. The data were reduced with the SAINT software⁶ to give the hkl file

- (1) (a) Bloomquist, D. R.; Willett, R. D. *Coord. Chem. Rev.* **1982**, *47*, 125. (b) Bloomquist, D. R.; Pressprich, M. R.; Willett, R. D. *J. Am. Chem. Soc.* **1988**, *110*, 7391. (c) Haddad, S. F.; Pickardt, J. *Transition Met. Chem.* **1993**, *18*, 377.
- (2) (a) Willett, R. D.; Ferraro, J. R.; Choca, M. *Inorg. Chem.* **1974**, *13*, 2919. (b) Scott, B.; Willett, R. D. *J. Am. Chem. Soc.* **1991**, *113*, 5253.
- (3) Halvorson, K.; Patterson, C.; Willett, R. D. *Acta Crystallogr.* **1990**, *B46*, 508.

- (4) (a) Bloomquist, D. R.; Willett, R. D.; Dodgen, H. W. *J. Am. Chem. Soc.* **1981**, *103*, 2610. (b) Roberts, S. A.; Bloomquist, D. R.; Willett, R. D.; Dodgen, H. W. *J. Am. Chem. Soc.* **1981**, *103*, 2603. (c) Wei, M.; Willett, R. D. *Inorg. Chem.* **1996**, *35*, 5781.
- (5) SMART, Software for the CCD Detector System, version 4.045; Bruker AXS, Inc.: Madison, WI, 1996.
- (6) SAINT, Software for the CCD Detector System, version 4.035; Bruker AXS, Inc., Madison, WI, 1996.

Table 1. Crystal Data and Structure Refinement for the Two Polymorphs of $(\text{Me}_2\text{NpyH})_2\text{CuCl}_4$

	green phase	yellow phase
formula	$\text{C}_{14}\text{H}_{22}\text{Cl}_4\text{CuN}_4$	$\text{C}_{14}\text{H}_{22}\text{Cl}_4\text{CuN}_4$
fw	451.70	451.70
space group	<i>P1</i>	<i>C2/c</i>
<i>a</i> /Å	7.7013(4)	11.973(3)
<i>b</i> /Å	8.7917(4)	12.522(3)
<i>c</i> /Å	15.9492(7)	14.523(3)
α /deg	84.7480(10)	90
β /deg	84.7100(10)	113.861(13)
γ /deg	66.3510(10)	90
<i>V</i> /Å ³	983.22(8)	1991.3(8)
<i>Z</i>	2	4
ρ_{calc} /Mg m ⁻³	1.526	1.507
<i>T</i> /K	298	298
μ /mm ⁻¹	1.657	1.636
<i>F</i> (000)	462	924
λ (Mo <i>K</i> α)/Å	0.710 73	0.710 73
reflns measd/unique	4403/2761	4341/1426
merging <i>R</i>	<i>R</i> (int) = 0.0185	<i>R</i> (int) = 0.0326
transm: max/min	0.862/0.614	0.432/0.322
<i>R</i> 1, ^a (<i>I</i> > 2 σ /all data)	0.0349/0.0418	0.0334/0.0357
<i>wR</i> 2, ^b (<i>I</i> > 2 σ /all data)	0.0848/0.0898	0.0943/0.0864

$$^a R1 = \sum ||F_o| - |F_c|| / \sum |F_o|. \quad ^b wR2 = \{ \sum [w(F_o^2 - F_c^2)^2] / \sum [w(F_c^2)^2] \}^{1/2}$$

Table 2. Bond Lengths [Å] and Angles [deg] for $(\text{Me}_2\text{NpyH})_2\text{CuCl}_4^a$

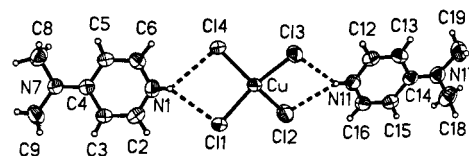
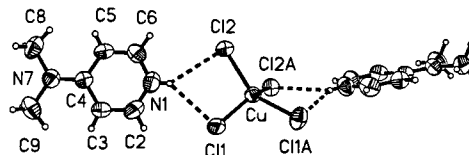
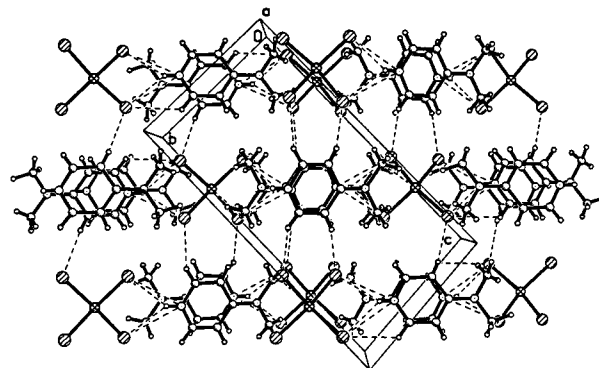
Green Phase			
Cu—Cl(1)	2.2636(8)	Cl(1)—Cu—Cl(2)	93.53(3)
Cu—Cl(2)	2.2467(9)	Cl(1)—Cu—Cl(3)	150.14(4)
Cu—Cl(3)	2.2556(9)	Cl(1)—Cu—Cl(4)	93.67(3)
Cu—Cl(4)	2.2466(8)	Cl(2)—Cu—Cl(3)	93.53(3)
		Cl(2)—Cu—Cl(4)	149.29(5)
		Cl(3)—Cu—Cl(4)	94.92(3)
N(1)—Cl(1)	3.238(3)	N(1)—H(1)—Cl(1)	145(4)
N(1)—Cl(4)	3.277(3)	N(1)—H(1)—Cl(4)	138(4)
N(11)—Cl(2)	3.261(3)	N(2)—H(2)—Cl(2)	137(4)
N(11)—Cl(3)	3.281(3)	N(2)—H(2)—Cl(3)	144(4)
Yellow Phase			
Cu—Cl(1)	2.2416(8)	Cl(1)#1—Cu—Cl(1)	97.22(5)
Cu—Cl(2)	2.2552(8)	Cl(1)—Cu—Cl(2)#1	139.91(3)
		Cl(1)—Cu—Cl(2)	95.26(3)
		Cl(2)#1—Cu—Cl(2)	99.23(5)
N(1)—Cl(1)	3.265(3)	N(1)—H(1)—Cl(1)	141(4)
N(1)—Cl(2)	3.289(3)	N(1)—H(1)—Cl(2)	142(4)

^a Symmetry transformations used to generate equivalent atoms: (#1) $-x, y, -z + 1/2$.

corrected for Lp/decay. The absorption correction was performed using the SADABS⁷ program. The structures were solved by the direct method using the SHELX-90⁸ program and refined by the least-squares method on *F*², SHELXL-93,⁹ incorporated in SHELXTL, version 5.03.¹⁰ Hydrogen atoms, with the exception of the methyl hydrogen atoms in the yellow phase, were located from difference syntheses and their positional and isotropic thermal parameters refined. All non-hydrogen atoms are refined anisotropically. Table 1 summarizes the most important structural and refinement parameters, while important distances and angles in the two compounds are given in Table 2. Figures 1 and 2 illustrate the molecular species for the two compounds.

Structure Description

The structures of the two isomorphs both contain the same basic structural unit that consists of a CuCl_4^{2-} anion bonded

**Figure 1.** Illustration of the $(\text{C}_7\text{H}_{11}\text{N}_2)_2\text{CuCl}_4$ molecular unit in the green phase. Thermal ellipsoids are presented at the 50% probability level.**Figure 2.** Illustration of the $(\text{C}_7\text{H}_{11}\text{N}_2)_2\text{CuCl}_4$ molecular unit in the yellow phase. Thermal ellipsoids are presented at the 50% probability level.**Figure 3.** Partial view of the packing in the green phase, as viewed from the *a* direction.

by two organic cations. The $(\text{C}_7\text{H}_{11}\text{N}_2)_2\text{CuCl}_4$ molecular units are built through the formation of bifurcated $\text{N}\cdots\text{H}\cdots\text{Cl}$ hydrogen bonds from the pyridinium nitrogen atoms to two of the cis chlorine atoms on the anions, as seen in Figures 1 and 2. The average $\text{N}\cdots\text{Cl}$ distances are only slightly longer in the yellow phase (3.281(1) Å) than in the green phase (3.262(2) Å). This difference in the average $\text{N}\cdots\text{Cl}$ distances is less than the spread in the distances (0.05 Å). The $\text{H}\cdots\text{Cl}$ distances range from 2.59(4) to 2.68(4) Å with the $\text{N}\cdots\text{H}\cdots\text{Cl}$ angles lying between 136(2)° and 145(2)° in the green phase. For the yellow phase the corresponding values average 2.67 Å and 142°.

The most obvious difference in conformation between the two phases is the orientation of the planes of the cations relative to the CuCl_4^{2-} anions. This can be seen by comparison of Figure 1 with Figure 2, where both views are normal to the plane of the pyridine ring of the left-hand cation. In the green phase, the cations are essentially coplanar with the CuCl_2 planes for the chlorine atoms involved in the hydrogen bond. The two independent dihedral angles between the cation planes and the relevant CuCl_2 planes are 9.4(1)° and 10.4(1)° in the green phase. This conformation is stabilized by electrostatic interactions between the *o*-hydrogen atoms of the pyridinium rings and the chloride ions of the anion. The $\text{H}\cdots\text{Cl}$ distances average 2.98 Å (range 2.8–3.1 Å), and the $\text{C}\cdots\text{H}\cdots\text{Cl}$ angles average 120° (range 116–126°). In the yellow phase, the planes of the cations are folded relative to the CuCl_2 planes and the dihedral angle has opened up to 31.2(1)°. Now the $\text{H}\cdots\text{Cl}$ distances have increased to 3.08 Å, average, and the $\text{C}\cdots\text{H}\cdots\text{Cl}$ angles closed to about 116°. For the green phase, the dihedral angle of 41.99(3)° between the two CuCl_2 planes gives a dihedral angle between the two pyridine rings of the molecular species of 36.9-

- (7) SADABS, Program for absorption correction for area detectors; Bruker AXS, Inc.: Madison, WI, 1996.
 (8) Sheldrick, G. M. SHELXS-90, Program for the Solution of Crystal Structure; University of Göttingen: Göttingen, Germany, 1986.
 (9) Sheldrick, G. M. SHELXL-97, Program for the Refinement of Crystal Structure; University of Göttingen: Göttingen, Germany, 1997.
 (10) SHELXTL, Program Library for Structure Solution and Molecular Graphics, PC version 5.10; Bruker AXS, Inc.: Madison, WI, 1997.

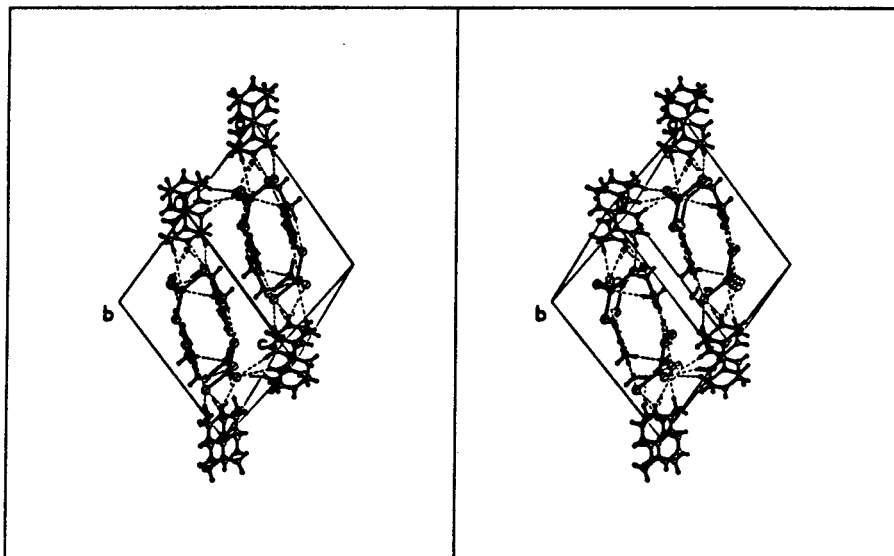


Figure 4. Stereoscopic view of the packing in the yellow phase, as viewed from the (1 1 0) direction.

(1)°. For the yellow phase, the dihedral angle is now 55.25(3)° between the two CuCl_2 planes and the dihedral angle between the pyridine rings is 79.1(1)°. This has important consequences on the packing, as discussed below.

Another significant difference in the two structures is the packing of the molecular species. In the green phase, the packing is extremely efficient. The $(\text{C}_7\text{H}_{11}\text{N}_2)_2\text{CuCl}_4$ species form interdigitated layers lying in the ab plane, as seen in Figure 3. Via this interdigitation, the pyridinium rings stack directly atop each other, as can also be clearly seen in Figure 3. The separations between adjacent pyridinium ring planes for ring 1 (containing N(1)) alternate between values of 3.65(1) and 3.47(1) Å, while for ring 2 (containing N(11)) the inter-ring distances are shorter, 3.40(1) and 3.46(1) Å. As can also be seen in Figure 3, the ring C–H bonds line up so that they are pointed toward Cl atoms in adjacent layers. This leads to a number of short $\text{H}\cdots\text{Cl}$ contacts with distances generally in the 3.0–3.2 Å range and with C–H \cdots Cl angles varying from roughly 130° to 170°. These electrostatic interactions presumably help provide three-dimensional stability. Similarly, a number of similar interactions occur within the layers with some of the $\text{H}\cdots\text{Cl}$ contacts being as short as 2.8 Å.

In the higher symmetry yellow phase, the larger twist between the planes of the two cation rings hydrogen-bonded to the CuCl_4^{2-} anions prevents the formation of a layer structure. Instead, symmetry-equivalent interdigitated stacks run parallel to both the (1 1 0) and (1 $\bar{1}$ 0) directions, as illustrated in the stereoscopic view given in Figure 4. In this view, which is from roughly the (1 1 0) direction, a (1 $\bar{1}$ 0) stack is running horizontally from the lower right to the upper left while portions of four sets of (1 1 0) stacks are shown that propagate in the vertical direction. A half-dozen different C–H \cdots Cl contacts exist with distances between 2.75 and 3.0 Å. Given the negligible differences in the N–H \cdots Cl hydrogen-bonding interactions in the two phases, it is clearly these C–H \cdots Cl electrostatic interactions that account for the structural differences of the two polymorphs.

The conformational difference in the two structures that is related to the color differences in the two phases is the extent of distortion of the CuCl_4^{2-} anions. In both phases, the anions assume a compressed tetrahedral geometry of approximate D_{2d} symmetry, consistent with the anticipated distortions precipitated by the Jahn–Teller effect. These distortions are typically

measured by the average value of the trans Cl–Cu–Cl angle, which would be 109.5° for the tetrahedral limit and 180° for the square planar end member.³ This trans angle is 10° larger in the green phase (149.7(4)°, average) compared with the angle in the yellow phase (139.91(3)°). The observed color change between the two phases is consistent with results from previous studies of the electronic spectra of the CuCl_4^{2-} species where orange \leftrightarrow yellow \leftrightarrow green color progressions is observed as the anion distortion progresses from the tetrahedral to square planar limit.³ This color change is primarily due to a blue shift of the first Cl \rightarrow Cu charge-transfer transition, which lies close to the UV/visible boundary of the spectrum. That shift is due to an increased splitting in the primarily d orbital levels as the anion approaches the square planar limit, which in turn causes the energy of the half-occupied MO level to increase.

The CuCl_4^{2-} anions do not deviate significantly from ideal D_{2d} geometry in either phase. In addition, the Cu–Cl bond distances are nearly identical in the two phases, averaging 2.25(3) Å in the green phase and 2.248(7) Å in the yellow phase. In the yellow phase, the anion has C_2 symmetry so that both trans angles are identical, but in the lower symmetry anion in the green phase, these two angles differ only by 0.84(3)°.

The geometry at the amine nitrogen is planar, indicating significant π delocalization between the pyridine ring and the amine nitrogen. This is substantiated by the short amine nitrogen–ring carbon bond distances (1.335(8) Å, average), which are identical to the ring C–N distances (1.335(5) Å, average). The differences in the two structures are primarily in the packing of these units, with substantial conformational changes accompanying the two different packing arrangements.

Discussion

While structural phase transitions in general and thermochromic transitions in particular are quite common in copper(II) halide salts and complexes, the mechanism (driving force) for the transition in this compound appears to be different from previous systems studied. For A_2CuX_4 salts of the so-called β - K_2SO_4 structure class where A is a small, non-hydrogen-bonding cation such as Me_4N^+ ,¹¹ Me_4P^+ ,¹² Me_3EtN^+ ,¹³ and $\text{Me}_2\text{Et}_2\text{N}^+$,¹³ multiple phase transitions are usually observed. These are associated with the onset of librational disorder of the cations as well as the CuX_4^{2-} anions.

However, with hydrogen-bonding cations, the phase transitions are usually associated with a weakening and disordering of the N–H···X hydrogen bonds with associated disorder of the organoammonium cations. Thus, in (Et₂NH₂)₂CuCl₄, the green ↔ yellow thermochromic transition is associated with the onset of disorder of the diethylammonium groups and a concomitant weakening of the N–H···Cl hydrogen bonding.^{1b} This latter factor increases the electrostatic repulsion between the halide ion in the CuCl₄²⁻ anions, forcing an increased distortion toward tetrahedral geometry. A similar behavior is observed in (φ-C₂H₄NH₂Me)₂CuCl₄, where disorder of the cations are observed in the high-temperature yellow form.¹⁴ A thermochromic copper(II) chloride salt in which disorder of the cation does not appear to play a role is [*N*-(2-ammoniothy)-morpholinium]CuCl₄.¹⁵ Two different polymorphs of this compound exist at room temperature, and no interconversion is observed upon heating to the decomposition temperature. The green phase in this compound contains both planar and distorted tetrahedral CuCl₄²⁻ anions, while the yellow phase contains only distorted tetrahedral anions. No disorder of the substituted morpholinium cations is reported for either phase (although no thermal parameters are reported, so it is not possible to look for evidence of differences of librational motions). However, the hydrogen-bonding networks are significantly rearranged between the two polymorphs, so the connectivity in the two structures is very different.

In another group of compounds, the phase changes are associated with a change in the extent of aggregation of the

inorganic moieties. For [(CH₃)₂CH₂NH₃]₂CuCl₄,^{4a} the green ↔ yellow phase transition is again associated with the disorder of the organoammonium ion. However, in this case, the disorder causes a breakup of the polymeric structure present in the low-temperature (green) phase and results in the formation of isolated distorted tetrahedral CuCl₄²⁻ anions in the high-temperature phase. For several other systems, such as C₄H₅NCuCl₃^{4c} and (CH₃)₂CH₂NH₃CuX₃^{4c,11} (X = Cl, Br), the thermochromism again appears to be driven by disorder of the organic cation. In these cases, the open five-coordinate (CuX₃)_{*n*}^{*n-*} structure collapses to a six-coordinate chain structure. Here, the Cu(II) halide lattice compensates for the weakening of the N–H···X interactions by the formation of new Cu–X···Cu interactions.

In contrast to the thermochromic materials discussed above, for the piezochromic salt [(C₃H₇)₄N]₂Cu₂Br₆,^{2b} no change occurs in the geometry of the copper bromide moiety. Rather, disorder of the cations simply leads to a new packing arrangement for the lattice and differences in the polarization properties of the electronic transitions lead to a change in color of the crystal.

In the system delineated in this paper, no significant change in hydrogen bonding occurs in the phase transition. In fact, the (C₇H₁₁N₂)₂CuCl₄ structural unit remains intact, with the only change being a greater twist of the plane of the pyridine rings of the cations relative to the CuCl₄²⁻ anion in the yellow phase. So the thermochromism is not associated with the onset of disorder of the organic cations. Rather, the yellow phase has a different packing scheme associated with the rearrangement of the C–H···Cl interactions. This packing arrangement forces the CuCl₄²⁻ anion to distort further toward a tetrahedral geometry, producing the color change.

Acknowledgment. The use of the Single Crystal Diffraction Facility at the University of Idaho is greatly appreciated. Partial support was obtained from The Deanship of Academic Research of The University of Jordan. The partial support of ACS-PRF 34779-AC5 is acknowledged.

Supporting Information Available: An X-ray crystallographic file in CIF format for the two polymorphs of (C₇H₁₁N₂)₂CuCl₄. This material is available free of charge via the Internet at <http://pubs.acs.org>.

IC000613C

- (11) (a) Clay, R.; Murray-Rust, J.; Murray-Rust, P. *Acta Crystallogr.* **1975**, *B31*, 289. (b) Asahi, T.; Hasebe, K.; Gesi, K. *J. Phys. Soc. Jpn.* **1988**, *57*, 4219. (c) Gesi, K.; Perret, J. *Phys. Soc. Jpn.* **1988**, *57*, 3698. (d) Lopez-Echarri, A.; Ruiz-Larrea, I.; Tello, M. J. *Phys. Status Solidi B* **1989**, *154*, 143. (e) Gomez-Cuevas, A.; Tello, M. J.; Fernandez, J.; Lopez-Echarri, A.; Herreros, J.; Couzi, M. *J. Phys. C* **1983**, *16*, 473.
- (12) (a) Bednarz, G.; White, M. A.; Pressprich, M. R.; Willett, R. D. *Phys. Rev. B* **1994**, *49*, 832. (b) Madariaga, G.; Alberdi, M. M.; Zuniga, F. J. *Acta Crystallogr.* **1990**, *C46*, 2263. (c) Pressprich, M. R. Ph.D. Thesis, Washington State University, Pullman, WA, 1990.
- (13) Willett, R. D.; Wei, M. *Phys. Chem. Solids* **2000**, *61*, 2025.
- (14) Harlow, R. L.; Wells, W. J.; Watt, G. W.; Simonsen, S. H. *Inorg. Chem.* **1974**, *13*, 2106.
- (15) Battaglia, L. P.; Bonamartini-Corradi, A.; Marcotrigiano, G.; Menabue, L.; Pellacani, G. C. *Inorg. Chem.* **1982**, *21*, 3919.